Research Papers
Issue RP0248
December 2014

ANS – Numerical Applications and Scenarios Division

CMCC–CESM–NEMO: toward the new CMCC Earth System Model

By **Pier Giuseppe Fogli**
Centro Euro-Mediterraneo sui Cambiamenti Climatici (CMCC)
piergiuseppe.fogli@cmcc.it

and **Dorotea Iovino**
Centro Euro-Mediterraneo sui Cambiamenti Climatici (CMCC)
dorotea.iovino@cmcc.it

SUMMARY This report describes the physical core of the new CMCC Earth System Model CMCC–CESM–NEMO. The model is largely based on the Community Earth System Model (CESM) project developed at the National Center for Atmospheric Research (NCAR). The ocean component of the CESM model has been replaced by the Nucleus for European Modelling of the Ocean (NEMO) general circulation model, developed by an European consortium of modelling centers of which the CMCC is an active member. An overview of the CMCC–CESM–NEMO model is provided, together with a detailed description of the integration of NEMO into CESM and of the design of the physical coupling interface.

The research leading to these results has received funding from the Italian Ministry of Education, University and Research and the Italian Ministry of Environment, Land and Sea under the GEMINA project

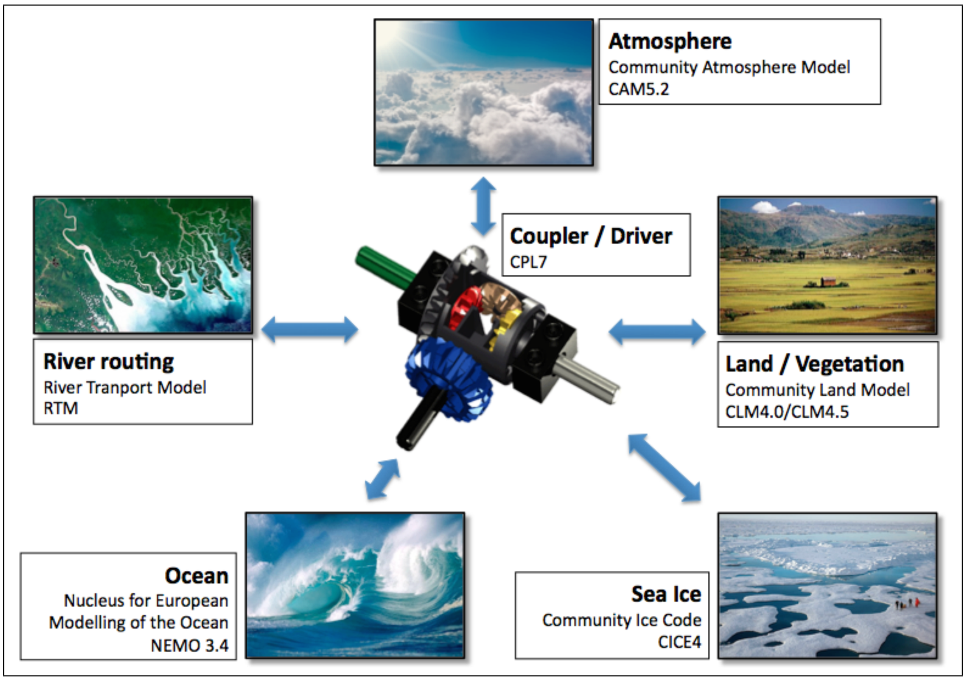

02

1. INTRODUCTION

The term Earth System refers to the interacting atmosphere, ocean, land surface, and sea ice, which comprise the "physical climate system", along with the biogeochemical processes that interact with this physical system. Numerical modeling of the Earth System is an important research and development topic with practical applications in atmospheric, oceanic, environmental forecasting, and climate science. It is recognized that the vulnerability to climate change will only increase. That results in an increasing need to improve our knowledge on climate variability. Development of the Earth System Models (ESMs) is determinant to address scientific hypothesis on climate and environmental change and to investigate the complex interactions within the Earth system. While Climate models describe the physics of the atmosphere, ocean, and the land surface, ESMs are a new type of global climate models with the added capability to explicitly represent biogeochemical processes that interact with the physical climate and so alter its response to forcing such as that associated with human caused emissions of greenhouse gases. Earth System modeling is an interdisciplinary enterprise that provides information on how biological processes and climate relates and will change in the future. ESMs are composed of model components that simulate individual parts of the climate system and the exchange of energy, mass and momentum between these parts.

The Euro-Mediterranean Centre on Climate Change (CMCC) is highly involved in improving the understanding of the mechanisms of climate variability, its causes and its impacts. CMCC is one of the modeling centers that contributed to the Coupled Model Intercomparison Project Phase 5 (CMIP5), used in support of the Fifth Assessment Report of the IPCC. For the upcoming H2020 program starting in Europe and the next contribution to the sixth phase of the CMIP project, CMCC has designed a new earth system model that integrate the interactions of atmosphere, ocean, land, ice, and biosphere in order to estimate the state of global climate under a wide variety of conditions. The physical core of the new CMCC's Earth System Model is largely based on the Community Earth System Model (CESM) project operated at the National Center for Atmospheric Research (NCAR) on behalf of the University Corporation for Atmospheric Research (UCAR) in USA, but differs from the latter in particular by the oceanic component. CMCC, as a member of the NEMO consortium, takes an active part in developing and maintaining the NEMO-OPA (Nucleus for European Modelling of the Ocean, Océan Parallélisé) Ocean General Circulation Model. That motived us in replacing the CESM ocean model and integrating NEMO into the system. This change and the ongoing development of the biogeoghemical component on top of the physical core provide the necessary model diversity desired for the sixth phase of the CMIP project.

This report describes in details the physical core of the so-called CMCC-CESM-NEMO model and its implementation. It is organized as follow. Section 2 gives an overview of the new model. Section 3 discuss the choices made to integrate NEMO into the CESM model. Finally, Section 4 describe in detail the physical coupling interface and its validation.

2. OVERVIEW OF THE CESM MODEL

The CMCC–CESM–NEMO is a coupled climate model for simulating Earth's system past, present, and future climate states. It consists of several independent model components simultaneously simulating the Earth's atmosphere, ocean, land, land ice and sea ice, in concert with a central coupler/driver component that controls the synchronization and data exchange.
Like the CESM system, CMCC–CESM–NEMO can be configured in a number of different ways from both a science and technical perspective and can be efficiently run on a number of different hardware platforms. It supports many resolutions and has the flexibility to set up simulations with different component configurations and parallel decompositions, which allow it to run from a single model in standalone forced configuration to the fully coupled system. Indeed, each model component may have "active", "data", "dead" or "stub" version allowing for a variety of "plug and play" combinations. An active component is the fully prognostic model. A data component is a model which cycles input data read from files, providing forcings or boundary conditions for the other components. A dead component generates scientifically invalid data and exists only for technical system testing. Finally, a stub component satisfy interface requirements when the component is not needed.
Figure 1 shows a schematic of the CMCC–CESM–NEMO model components. The CMCC-CESM-NEMO model is based on CESM version 1.1.2 [16, 7]. An overview of the CESM model components follows. A detailed description is given in Hurrell et al. (2012) [16] and references therein.

Figure 1:
Schematic of the CMCC–CESM–NEMO model components.

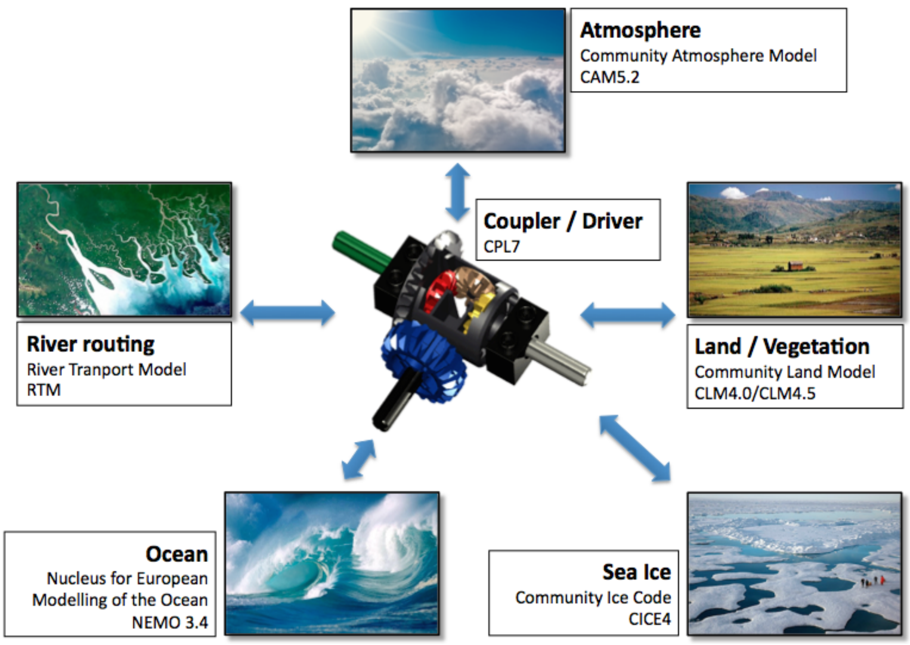

The atmospheric component is the Community Atmosphere Model (CAM–5.2). CAM5 can be configured to use a spectral transform, a finite volume or a finite elements dynamical core. A description of the treatment for stratiform cloud formation, condensation, and evaporation (macrophysics) is given in Neale et al. (2010) [27]. A two-moment microphysical parameterization (Morrison and Gettelman 2008 [26]; Gettelman et al. 2008 [8]) is used to predict the mass and number of smaller cloud particles (liquid and ice), while the mass and number of larger precipitating particles (rain and snow) are diagnosed. Cloud microphysics is coupled to a modal aerosol treatment (Liu et al. 2012 [24]; Ghan et al. 2012 [9]) that predicts the aerosol mass and number of internal mixtures of black and organic carbon, dust, sea salt, and sulfate aerosols. A two-stream correlated-k distribution Rapid Radiative Transfer Model for GCMs (RRTMG; Iacono et al. 2008 [17]) is used to calculate the radiative fluxes and heating rates for gaseous and condensed atmospheric species. A statistical technique is used to represent subgrid-scale cloud overlap (Pincus et al. 2003 [31]). New moist turbulence (Bretherton and Park 2009 [2]) and shallow convection parameterization schemes (Park and Bretherton 2009 [30]) provide substantial improvements to the simulation of shallow clouds in the boundary layer.

The land component is the Community Land Model (CLM4.0) (Lawrence et al. 2011a [21]; Oleson et al. 2010 [29]). The Community Land Model (CLM) is designed to represent and enable study of the physical, chemical, and biological processes by which terrestrial ecosystems affect and are affected by climate across a variety of spatial and temporal scales. The central theme is that terrestrial ecosystems, through their cycling of energy, water, chemical elements, and trace gases, are important determinants of climate. The land surface is a critical interface through which climate change impacts humans and ecosystems and through which humans and ecosystems can effect global environmental change. New features relative to previous versions of CLM include a prognostic carbon–nitrogen (CN) model (Thornton et al. 2007 [38]) an urban canyon model (Oleson et al. 2008 [28]) and a transient land cover and land use change capability, including wood harvest (Lawrence et al. 2012a [20]). A revised snow model incorporates the Snow, Ice, and Aerosol Radiation (SNICAR) model (Flanner et al. 2007 [6]). SNICAR includes aerosol deposition of black carbon and dust (either prescribed or determined prognostically by CAM), grain-size dependent snow aging, and vertically resolved snowpack heating. Dust is mobilized from the land by wind (Zender et al. 2003 [40]) and passed to the atmospheric aerosol model. The representation of permafrost is significantly improved in CLM4 (Lawrence et al. 2011b [22]). The dynamic global vegetation model in CLM3 is merged with CN in CLM4 (Gotangco Castillo et al. 2012 [10]). Finally, CLM4 possesses an interactive crop management model (Levis et al. 2012 [23]) and an irrigation scheme (Sacks et al. 2009 [34]). The crop model is based on agricultural version of the Integrated Biosphere Simulator (Agro-IBIS; Kucharik and Brye 2003 [18]) and includes parameters for corn, soybean, and temperate cereals. When irrigation is enabled, the cropland area of each grid cell is divided into an irrigated and unirrigated fraction according to a dataset of areas equipped for irrigation. Biogenic volatile organic compound emissions from vegetation are also calculated and passed to CAM.

The sea ice component is version 4 of the Community Ice CodE (CICE4) (Hunke and Lipscomb 2008 [14]) which use the same horizontal grid of the ocean model. It includes the thermodynamics of Bitz and Lipscomb (1999) [1], the elastic–viscous–plastic dynamics of Hunke and Dukowicz (2002) [15], and a subgrid-scale representation of ice thickness distribution following Thorndike et al. (1975) [37] and Rothrock (1975) [32]. As documented in Holland et al. (2012) [13], the most notable improvements in the sea ice component of CESM compared to earlier model versions includes a multiple-scattering shortwave radiation treatment (Briegleb and Light 2007) [3] and associated capabilities to simulate explicitly melt pond evolution and the deposition and cycling of aerosols (dust and black carbon) within the ice pack. These new capabilities influence both the mean climate state and simulated climate feedbacks at high latitudes (Holland et al. 2012) [13].

All the components are synchronized by the CESM coupler/driver (cpl7) (Craig et al. 2012 [4]) The coupling architecture provides plug and play capability of data and active components and includes a user-friendly scripting system and informative timing utilities. Together, these tools enable a user to create a wide variety of out-of-the box experiments for different model configurations and resolutions and also to determine the optimal load balance for those experiments to ensure maximal throughput and efficiency.

3. INTEGRATING NEMO INTO CESM

A brief overview of the NEMO model is provided in this section, with an emphasis on the global configurations commonly used at CMCC. Following, a discussion of the choices made to integrate NEMO into the CESM model is presented. Finally, the fields required to couple the ocean component to the rest of the system are described in order to identify missing fields. This will serve as a base for the physical coupling interface described in detail in the next section.

3.1 OVERVIEW OF THE NEMO MODEL

The Nucleus for European Modelling of the Ocean (NEMO) [25] is a flexible tool for studying the ocean and its interactions with the other components of the Earth climate system over a wide range of space and time scales. The NEMO model solves the primitive equations subject to the Boussinesq, hydrostatic and incompressibility approximations. The prognostic variables are the three velocity components, the sea surface height, the potential temperature and the practical salinity. A summary of the model configuration used at CMCC is given.
The ocean component we used is based on version 3.4 of NEMO. In the horizontal direction the model uses a nearly isotropic curvilinear orthogonal grid with an Arakawa C–type three-dimensional arrangement of variables. For our global configurations, we use tripolar ORCA-like grids (based on Mercator projection), which have a pole in the Southern Hemisphere collocated with the geographic South Pole and two poles placed on land in the Northern Hemisphere (in Siberia and Canada) in order to overcome the North Pole singularity. Poleward of 20°N, the two poles introduce a weak anisotropy over the ocean areas. Up to now, the CMCC Earth System has been run in two configurations: a lower 1° resolution (ORCA1) and a higher, eddy-permitting, 1/4° resolution. The low resolution configuration (ORCA1) includes an additional meridional refinement in the equatorial region (20°S–20°N).
The model uses a filtered linear free-surface formulation, where lateral fluxes of volume, tracers and momentum are calculated using fixed reference ocean surface height. The time integration scheme used is a Robert–Asselin filtered leap-frog for non-diffusive processes and a forward (backward) scheme for horizontal (vertical) diffusive processes. The linear free-surface is integrated in time implicitly using the same time step.
The model uses a non linear equation of state. Tracers advection uses a Total Variance Dissipation (TVD) scheme while momentum advection is formulated in vector invariant form using an energy and enstrophy conserving scheme. The vertical physics is parameterized using a Turbulent Kinetic Energy (TKE) closure scheme plus parameterizations of double diffusion, Langmuir cell and surface wave breaking. An enhanced vertical diffusion parameterisation is used in regions where the stratification becomes unstable. Tracers lateral diffusion uses a diffusivity coefficient scaled according to the grid spacing and is parameterized by an iso-neutral Laplacian (bi-Laplacian) operator in the low (high) resolution configurations. An additional eddy-induced velocity is applied in the low resolution configuration using a spatially and temporally varying coefficient. Lateral viscosity uses a space varying coefficient and is parameterized by a horizontal Laplacian (bi-Laplacian) operator in the low (high) resolution configuration. Free-slip boundary conditions are applied at the ocean lateral boundaries. At the ocean floor, a bottom intensified tidally driven mixing, a diffusive bottom boundary layer scheme and a non-linear bottom friction are applied. No geothermal heat flux is

applied through the ocean floor. The shortwave radiation from the atmosphere is absorbed in the surface layers using RGB chlorophyll-dependent attenuation coefficients.

3.2 CHOICE OF THE HORIZONTAL GRID

The integration of NEMO into CESM requires choosing the horizontal grid used by the ocean and sea ice components. Two options are available:

- grids already supported by CESM (POP2 grids), adapting NEMO to use these grids
- the ORCA grid family, adding support specific for these grids into CESM

The former would require the creation of new grid coordinates, metrics, bathymetry, land–sea mask, initial and boundary conditions for NEMO, and eventualy some hand tuning concerning for example narrow straits, marginal seas and partial steps bottom topography. Since ORCA grids for the used resolutions are already availalbe at CMCC the latter would require just the creation of mapping files (interpolation weights) between the ORCA grid and the atmospheric grid, by means of the mapping tools provided by CESM. Given these considerations, using the ORCA grid has been judged to be the best solution in terms of amount of work and of ease and robustness of the implementation.

3.3 CHOICE OF THE SEA ICE MODEL

Given that both the NEMO and the CESM have their own sea ice component, is necessary to decide which one to use.
In the CESM infrastructure, each model component can be considered a separate stand alone model which communicates and exchanges data with the other components through the CPL7 coupler. Even though CESM uses a single executable strategy, the data exchange data among components is operated only through the coupler. Moreover, the physical coupling interface currently implemented in CESM requires that the sea ice model is responsible for the computation of fluxes of heat, mass and momentum with the atmosphere based on surface and near-surface conditions provided by the atmospheric model.
The NEMO-OPA ocean component is generally coupled to the Louvain-la-neuve Ice Model (LIM, version 2 or 3)[39], taht is implemented as a number of modules activated at compilation time through a CPP macro. The coupling between NEMO and LIM therefore does not require the presence of a coupler as they are part of the same executable and share the same memory. Both models are forced by the same atmospheric fluxes, which are computed using bulk formulæin forced mode or received by a coupler in coupled runs. Since LIM is designed to be forced by atmospheric fluxes, no flux computation is currently implemented in it.
This means that the inclusion of the LIM model in the CESM infrastructure currently requires a far greater effort with respect to the use of the CICE model already available in CESM. Indeed with the used NEMO version the inclusion of LIM in CESM would require the re-engineering of the sea ice module as a separate stand alone model and the implementation of the fluxes computation. On the other hand, the CICE model already supports the kind of tripolar grid used by NEMO and only needs the creation of the grid coordinates and metrics files and the land–sea mask file, consistent with the grid choice previously described.

Figure 2:
Grid staggering used by CICE (left) and NEMO (right) showing the location of tracers (T) and velocity (U, V) points with respect to the model grid cell. F points in NEMO indicate where vorticity is computed.

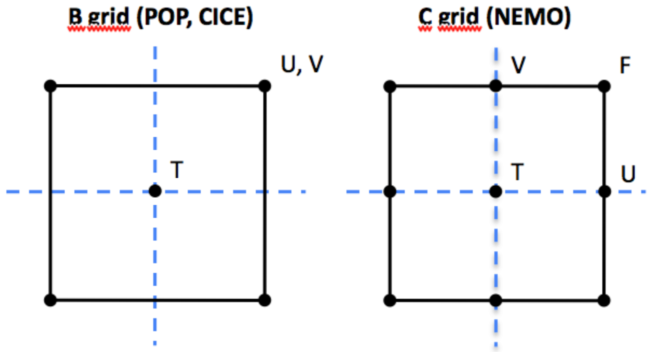

3.4 COUPLING FIELDS

To design the coupling interface between NEMO and the coupler, it is necessary to identify the fields expected and provided by each of them, in order to define which field is already available and which is missing and still needed to be added. Furthermore, for each field we need to know its units, sign convention and location with respect to grid staggering (central T points or velocity points).
Careful attention must be paid to the different grid staggering used by NEMO (C–grid) and CICE (B–grid), see Figure 2. In its current configuration, the coupler cannot associate more than one grid to each component model. As a consequence, all the exchanged fields are provided on the T grid. Fields located on a different grid needs to be interpolated on the T grid before being sent, while fields expected on a different grid must be interpolated from the T grid to the target grid upon receiving. NEMO already has routines/code for interpolating/shifting fields between T, U, V and F points, as well as for rotation along geographical coordinates or along local grid coordinates.
Tables 1, 2 and 3 document the field expected/provided by the CESM coupler and expected by NEMO respectively. For each field, its units, sign convention, grid location and source or target model component are indicated.
Concerning the fields the CESM model expects from the ocean component (Table 1), NEMO already is able to provide all of them except for the freezing/melting potential heat flux. The computation of this heat flux has been implemented in NEMO following the method used for the default CESM ocean component, POP2 Parallel Ocean Program (see Chap. 8.2 in POP2 Reference Manual [35]). Briefly, this heat flux accounts for sea ice formation when the sea water temperature falls below the freezing point, or potential melting of sea ice when the sea surface temperature is above the freezing point. It is required by CICE who converts it in newly formed sea ice or use it to melt already existing sea ice.
The sea surface horizontal velocity components need to be interpolated from the U and V grids to the T grid and rotated along the geographical coordinates before sending them to the coupler. The sea surface horizontal pressure gradient is computed from the sea surface height and do not require rotation because it's used by the sea ice component who shares the same horizontal grid.

Table 1
Fields expected from the ocean component by the cpl7 coupler

Field	Units	Positive	Grid	Target component
Sea Surface Zonal Horiz. Velocity	m/s	-	U→T+rot	Atm & Sea Ice
Sea Surface Meridional Horiz. Velocity	m/s	-	V→T+rot	Atm & Sea Ice
Sea Surface Temperature	K	-	T	Atm & Sea Ice
Sea Surface Salinity	ppt	-	T	Sea Ice
Sea Surface X Horiz. Pressure Gradient	m/m	-	T	Sea Ice
Sea Surface Y Horiz. Pressure Gradient	m/m	-	T	Sea Ice
Freezing/Melting Potential Heat Flux	W/m^2	Down	T	Sea Ice
CO_2 Flux	$Kg(CO_2)/m^2/s$	Down	T	Atm

Table 2
Fields provided to the ocean component by the cpl7 coupler

Field	Units	Positive	Grid	Source component
Surface Zonal Wind Stress	Pa	Down	T	Cpl (Atm, Ocn & Sea Ice)
Surface Meridional Wind Stress	Pa	Down	T	Cpl (Atm, Ocn & Sea Ice)
Freshwater Flux due to Snow	$Kg/m^2/s$	Down	T	Atm
Freshwater Flux due to Rain	$Kg/m^2/s$	Down	T	Atm
Freshwater Flux due to Evaporation	$Kg/m^2/s$	Down	T	Cpl (Atm, Ocn & Sea Ice)
Freshwater Flux due to Snow/Sea Ice Freezing/Melting	$Kg/m^2/s$	Down	T	Sea Ice
Salt Flux from Sea Ice	$Kg(S)/m^2/s$	Down	T	Sea Ice
Surface Shortwave Heat Flux	W/m^2	Down	T	Atm
Surface Downward Longwave Heat Flux	W/m^2	Down	T	Atm
Surface Upward Longwave Heat Flux	W/m^2	Down	T	Cpl (Atm, Ocn & Sea Ice)
Surface Sensible Heat Flux	W/m^2	Down	T	Cpl (Atm, Ocn & Sea Ice)
Surface Latent Heat Flux	W/m^2	Down	T	Cpl (Atm, Ocn & Sea Ice)
Heat Flux due to Snow/Sea Ice Melting	W/m^2	Down	T	Sea Ice
Sea Ice Fraction	0-1	-	T	Sea Ice
River Runoff	$Kg/m^2/s$	Down	T	River
Ice Runoff	$Kg/m^2/s$	Down	T	River
Sea Level Pressure	Pa	-	T	Atm
10m Wind Speed Squared	m^2/s^2	-	T	Cpl (Atm, Ocn & Sea Ice)
CO_2 Partial Pressure	ppmv	-	T	Atm

The flux of carbon dioxide is expected only when required by the particular experiment (e.g. when a biogeochemistry module is active).

Finally, regarding the fields that NEMO expects from the coupler (Table 3), CESM already is able to provide all of them (Table 2). Some of these fields are computed by the coupler itself through the NCAR bulk formulæ [19], using surface and near-surface conditions provided by different model components. Some variables need to be aggregated once received by NEMO in order to get the field actually used by the ocean. For example, the NEMO surface net non-solar heat flux is equivalent

Table 3
Fields expected by the NEMO model

Field	Units	Positive	Grid	Source component
Surface Zonal Wind Stress	Pa	-	T+rot➔U	Cpl (Atm, Ocn & Sea Ice)
Surface Meridional Wind Stress	Pa	-	T+rot➔V	Cpl (Atm, Ocn & Sea Ice)
Surface Wind Stress Module	Pa	-	T	Cpl (Atm, Ocn & Sea Ice)
10m Wind Speed	m/s	-	T	Cpl (Atm, Ocn & Sea Ice)
Surface Net Non-solar Heat Flux	W/m^2	Down	T	Cpl (Atm, Ocn & Sea Ice)
Surface Net Solar Heat Flux	W/m^2	Down	T	Cpl (Atm, Ocn & Sea Ice)
Evaporation-Precipitation Freshwater Flux	$Kg/m^2/s$	Up	T	Cpl (Atm, Ocn & Sea Ice)
Water Equivalent of Snow Precipitation	$Kg/m^2/s$	Up	T	Atm
Freshwater Flux due to River Runoff	$Kg/m^2/s$	Up	T	River
Salt Flux from Sea Ice	$PSU{\cdot}Kg/m^2/s$	Up	T	Sea Ice
Sea Level Pressure	Pa	-	T	Atm
CO_2 Partial Pressure	ppmv	-	T	Atm

to the sum of the net longwave radiation, the sensible heat flux, the latent heat flux, the heat flux associated to sea ice freezing/melting and the heat flux associated to melting of snow falling over the ocean and of the ice runoff.
All the fields whose source components are both the atmosphere and the sea ice are considered to be at the atmosphere–ocean or sea ice–ocean interface (i.e. under sea ice), so they already take into account sea ice processes. For example, the surface wind stress represents the weighted average between the atmospheric wind stress over open ocean and the ice–ocean stress under sea ice. Surface wind stresses, expected over the velocity points, need to be rotated along the local grid direction and interpolated from the T grid to the target velocity grid.

4. THE PHYSICAL COUPLING INTERFACE

The objective of the physical coupling interface is to exchange heat, mass and momentum between the different components of the climate model. This has to be done in a conservative way in order to avoid drifts in the coupled system. The conservation requirement is of paramount importance in climate modelling, where long multi-century simulations are usual and even a mild non-conservation can result in an unacceptable model drift.
The most delicate aspect in coupling an ocean model is its interaction with the sea ice component, because unlike at the air–sea interface, where only momentum, heat and freshwater are transfered, at the sea ice–ocean interface also sea salt is exchanged due to ice freezing and melting.
As pointed out by Roullet and Madec (2000) [33], the linear free surface implemented in NEMO does not perfectly conserve tracers. Nonetheless, this non-conservation is considered acceptable for climate modelling and represents a good compromise between the conservation requirement and the computational cost required by more sophisticated conservative implementations. The physical coupling inteface between NEMO and CICE is based on the work of Tartinville et al. (2001) [36], which represent an extension of [33] to a coupled ice–ocean model.

4.1 DESCRIPTION

Horizontal momentum is transfered from the atmosphere and sea ice to the ocean by the surface stresses, which represent a sea ice cover weighted average between the atmospheric wind stress over open ocean and of the ice–ocean stress under sea ice.
Transfer of heat is realized by different air–sea and ice–ocean processes. Figure 3 shows a schematic of the heat fluxes at the air–ocean–sea ice interface. The net heat flux at the ocean surface Q is given by:

$$Q = Q_{LW} \downarrow + Q_{LW} \uparrow + Q_{SW} + Q_L + Q_h - (P_{snow} + R_{ice}) \cdot L_f + Qice \quad (1)$$

where Q_{LW} is the longwave heat flux (downward and upward), Q_{SW} is the shortwave heat flux, Q_L is the latent heat flux, Q_h is the sensible heat flux, P_{snow} is the snow, R_{ice} is the ice runoff, L_f is the

Figure 3:
Schematic of the heat fluxes at the air–ocean–sea ice interface.

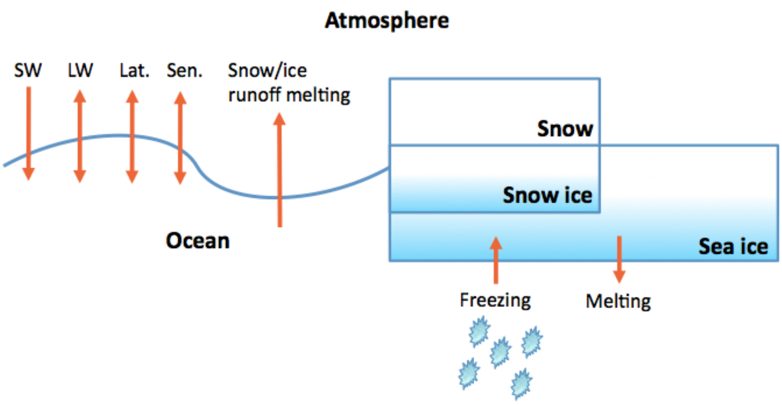

latent heat of fusion of the ice and Q_{ice} is the heat flux due to sea ice processes.
Here the Q_{ice} term consists of two contributions: the heat flux computed by NEMO associated to sea ice formation in the ocean, and the heat flux computed by CICE which takes into account the sea ice evolution.
The first term has been implemented in NEMO following the implementation in POP2 (see Chap. 8.2 in POP2 Reference Manual [35]). When the sea water temperature drops below its freezing point new sea ice is assumed to form. The sea water temperature is adjusted to the freezing point temperature and the resulting temperature difference is converted into an equivalent heat flux wto be sent to CICE, which in turn converts it in newly formed sea ice. While this flux term is diagnosed and stored by NEMO, it does not enter directly the surface temperature forcing because its effect is implicitly taken into account in the temperature adjustment, performed at the end of each time step. On the other hand, where the sea water temperature is above the freezing point, ea ice potentially melt. The temperature difference, converted to equivalent heat flux, is sent to CICE, without any temperature adjustment in the ocean. The portion of the melting potential actually used to melt ice is returned to NEMO at the subsequent coupling time step. At this point, NEMO adjusts its heat budget with this heat flux. This delay of one coupling time step is necessary because NEMO does not know if sufficient sea ice is available for melting.
Figure 4 shows a schematic of the mass fluxes at the air-ocean–sea ice interface. Mass exchanges have been implemented following Tartinville et al. (2001) [36] and are based on the following two considerations:

- The exchanges of freshwater between the sea ice and the ocean do not contribute to a modification of the pressure field in the ocean at a reference level
- The sea ice acts as a blanket that delays the dilution effect due to snow precipitation

Figure 4:
Schematic of the mass fluxes at the air–ocean–sea ice interface. Freshwater fluxes are denoted by blue and gray arrows, while salt fluxes are denoted by orange arrows. Modified after Tartinville et al. (2001) [36]

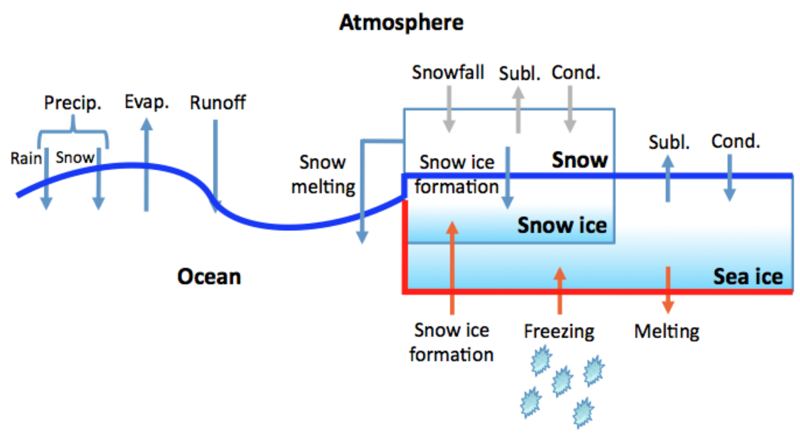

As a consequence, in order to distinguish between salt and freshwater fluxes, the following two rules are adopted:

- if liquid or solid water is added to or extracted from the ice–ocean system as a whole, then it is introduced as a freshwater flux (arrows crossing the **thick blue** line in Figure 4)
- if surface processes affect salinity without a net gain or loss of water for the ice–ocean system, then this internal exchange is converted into an equivalent salt flux that is applied to the ocean (arrows crossing the **thick orange** line in Figure 4)

This approach ensures that the mass exchange does contribute to the variation of the pressure field at a reference level, while the freshwater flux associated with sea ice melting and freezing does not. As a result, the sea ice acts as a negative salt reservoir inside the ice-ocean system. The effect on the seawater salinity of the snow falling over sea ice is delayed until this snow melts or is transformed into snow ice, at which point it is incorporated into the fluxes to the ocean. Only freshwater is taken into account when snow melts, while both freshwater and salt are incorporated into the ocean when it is transformed into snow ice. A drawback of this method is that also the effect on the ocean pressure field of the snow over sea ice is delayed until melting or snow ice conversion. As a result of this approach the surface freshwater (F_F) and salt (F_S) fluxes are:

- $$F_F = P - E + R - \rho_s \left(\frac{\partial h_s}{\partial t} \right)_{mlt,\ si} - \rho_i \left(\frac{\partial h_i}{\partial t} \right)_{subl,\ cond} \quad (2)$$
- $$F_S = \rho_i \left(S_o - S_i \right) \left(\frac{\partial h_i}{\partial t} \right)_{frz,\ mlt,\ si} \quad (3)$$

where P is the precipitation (both liquid and solid), E is the evaporation, R is the river runoff (both liquid and solid), ρ_s is the snow density, ρ_i is the sea ice density, h_s is the snow thickness over sea ice, h_i is the sea ice thickness, S_o is the sea water reference salinity, S_i is the sea ice reference salinity and the subscripts denote the involved processes (freezing, melting, snow ice formation, condensation and sublimation over sea ice).
This formulation differs from the one implemented between CICE and POP in the original CESM, due to the fact that POP uses a linear free surface with a varing first-level tickness, which ensures tracers conservation with the shortcoming of being more computationally expensive. As a consequence the freshwater and salt fluxes computed by CICE have been modified in order to compute those described above.

4.2 VALIDATION

The plug and play phylosophy of the CESM model can be exploited during both development and testing of new features. To test the new oceanic component all others components have been used in data version. This provides both a more controlled environment due to the absence of some of the feedbacks present in the fully coupled system and a computational advantage due to the absence of some of the expensive fully prognostic components.

Being one of the participating models to phase II of the Coordinated Ocean-ice Reference Experiments (COREs) (Griffies et al. 2009) [11], validation of the physical coupling interface of the CMCC–CESM–NEMO model has been done performing a coupled sea ice–ocean forced simulation.

The second phase of CORE (Griffies et al. 2012) [12] defines a protocol for performing global ocean–sea ice coupled simulations forced with common inter-annually varying atmospheric forcings (IAF), covering the 60-year period from 1948 to 2007 (Large and Yeager, 2009) [19]. Models were integrated for 300 years, corresponding to five cycles of the forcing data.

Analysis of the mean state of the North Atlantic Ocean for the 1°(ORCA1) global configuration of the CMCC–CESM–NEMO model are presented in Danabasoglu et al. 2014 [5]. Further analysis are at various stages of preparation and will be part of an on-line special issue of *Ocean Modelling*.

Validation and tuning of the fully coupled system is currently ongoing.

Results show that while some well known long-standing NEMO bias is still present, both the mean state and variability of the ocean–sea ice coupled system are well captured by the model.

One of the most importan aspects of the validation concerns the conservation of tracers in the ocean. This can be done comparing the tracer flux across the model boundaries reconstructed from the time rate of change of the global mean of the tracer, with the tracer flux actually seen by the model (see Appendix D.4 in [11]). Results show that the conservation error on the globally averaged temperature is of the order of 10^{-3} °C/century, while the conservation error on the globally averaged salinity is of the order of 10^{-4} PSU/century. These results confirm that the CMCC–CESM–NEMO model can be used for long term multi-century climate simulations.

Bibliography

[1] C. M. Bitz and W. H. Lipscomb. An energy-conserving thermodynamic model of sea ice. *J. Geophys. Res.: Oceans*, 104(C7):15669–15677, 1999. doi:10.1029/1999JC900100.

[2] C. S. Bretherton and S. Park. A new moist turbulence parameterization in the Community Atmosphere Model. *J. Climate*, 22(12):3422–3448, 2009. doi:10.1175/2008JCLI2556.1.

[3] B. Briegleb and B. Light. A Delta-Eddington multiple scattering parameterization for solar radiation in the sea ice component of the Community Climate System Model. NCAR Technical Note, NCAR/TN-472+ STR, National Center for Atmospheric Research, 2007. doi:10.5065/D6B27S71.

[4] A. P. Craig, M. Vertenstein, and R. Jacob. A new flexible coupler for earth system modeling developed for CCSM4 and CESM1. *Int. J. High Perform. Comput.*, 26(1):31–42, 2012. doi:10.1177/1094342011428141.

[5] G. Danabasoglu, S. G. Yeager, D. Bailey, E. Behrens, M. Bentsen, D. Bi, A. Biastoch, C. Böning, A. Bozec, V. M. Canuto, C. Cassou, E. Chassignet, A. C. Coward, S. Danilov, N. Diansky, H. Drange, R. Farneti, E. Fernandez, P. G. Fogli, G. Forget, Y. Fujii, S. M. Griffies, A. Gusev, P. Heimbach, A. Howard, T. Jung, M. Kelley, W. G. Large, A. Leboissetier, J. Lu, G. Madec, S. J. Marsland, S. Masina, A. Navarra, A. J. George Nurser, A. Pirani, D. S. y Mélia, B. L. Samuels, M. Scheinert, D. Sidorenko, A.-M. Treguier, H. Tsujino, P. Uotila, S. Valcke, A. Voldoire, and Q. Wang. North Atlantic simulations in Coordinated Ocean-ice Reference Experiments phase II (CORE-II). Part I: Mean states. *Ocean Modell.*, 73:76–107, 2014. doi:10.1016/j.ocemod.2013.10.005.

[6] M. G. Flanner, C. S. Zender, J. T. Randerson, and P. J. Rasch. Present-day climate forcing and response from black carbon in snow. *J. Geophys. Res.: Atmospheres*, 112(D11), 2007. doi:10.1029/2006JD008003.

[7] P. R. Gent, G. Danabasoglu, L. J. Donner, M. M. Holland, E. C. Hunke, S. R. Jayne, D. M. Lawrence, R. B. Neale, P. J. Rasch, M. Vertenstein, P. H. Worley, Z.-L. Yang, and M. Zhang. The Community Climate System Model Version 4. *J. Climate*, 24(19):4973–4991, 2011. doi:10.1175/2011JCLI4083.1.

[8] A. Gettelman, H. Morrison, and S. J. Ghan. A new two-moment bulk stratiform cloud microphysics scheme in the Community Atmosphere Model, version 3 (CAM3). Part II: Single-column and global results. *J. Climate*, 21(15):3660–3679, 2008. doi:10.1175/2008JCLI2116.1.

[9] S. J. Ghan, X. Liu, R. C. Easter, R. Zaveri, P. J. Rasch, J.-H. Yoon, and B. Eaton. Toward a minimal representation of aerosols in climate models: Comparative decomposition of aerosol direct, semidirect, and indirect radiative forcing. *J. Climate*, 25(19):6461–6476, 2012. doi:10.1175/JCLI-D-11-00650.1.

[10] C. K. Gotangco Castillo, S. Levis, and P. Thornton. Evaluation of the New CNDV Option of the Community Land Model: Effects of Dynamic Vegetation and Interactive Nitrogen on CLM4 Means and Variability. *J. Climate*, 25(11):3702–3714, 2012. doi:10.1175/JCLI-D-11-00372.1.

[11] S. M. Griffies, A. Biastoch, C. Böning, F. Bryan, G. Danabasoglu, E. P. Chassignet, M. H. England, R. Gerdes, H. Haak, R. W. Hallberg, et al. Coordinated Ocean-ice Reference Experiments (COREs). *Ocean Modell.*, 26(1):1–46, 2009. doi:10.1016/j.ocemod.2008.08.007.

[12] S. M. Griffies, M. Winton, B. Samuels, G. Danabasoglu, S. Yeager, S. Marsland, H. Drange, and M. Bentsen. Datasets and protocol for the CLIVAR WGOMD Coordinated Ocean-sea ice Reference Experiments (COREs). Technical Report 21, WCRP Report, 2012. URL: http://eprints.soton.ac.uk/350257/1/ICPO_184_%20Datasets%20and%20protocol%20for%20the%20CLIVAR%20WGOMD%20Coordinated%20Ocean-sea%20ice%20Reference%20Experiments%20%28COREs%29.pdf.

[13] M. M. Holland, D. A. Bailey, B. P. Briegleb, B. Light, and E. Hunke. Improved sea ice shortwave radiation physics in CCSM4: the impact of melt ponds and aerosols on Arctic sea ice. *J. Climate*, 25(5):1413–1430, 2012. doi:10.1175/JCLI-D-11-00078.1.

[14] E. Hunke and W. Lipscomb. CICE: The Los Alamos sea ice model, documentation and software, version 4.0, Los Alamos National Laboratory. Technical report, LA-CC-06-012, 2008.

[15] E. C. Hunke and J. K. Dukowicz. The elastic-viscous-plastic sea ice dynamics model in general orthogonal curvilinear coordinates on a sphere-incorporation of metric terms. *Mon. Wea. Rev.*, 130(7):1848–1865, 2002. doi:10.1175/1520-0493(2002)130\%3C1848:TEVPSI\%3E2.0.CO;2.

[16] J. W. Hurrell, M. M. Holland, P. R. Gent, S. Ghan, J. E. Kay, P. J. Kushner, J. F. Lamarque, W. G. Large, D. Lawrence, K. Lindsay, W. H. Lipscomb, M. C. Long, N. Mahowald, D. R. Marsh, R. B. Neale, P. Rasch, S. Vavrus, M. Vertenstein, D. Bader, W. D. Collins, J. J. Hack, J. Kiehl, and S. Marshall. The Community Earth System Model: A Framework for Collaborative Research. *Bull. Amer. Meteor. Soc.*, 94(9):1339–1360, 2013. doi:10.1175/BAMS-D-12-00121.1.

[17] M. J. Iacono, J. S. Delamere, E. J. Mlawer, M. W. Shephard, S. A. Clough, and W. D. Collins. Radiative forcing by long-lived greenhouse gases: Calculations with the AER radiative transfer models. *J. Geophys. Res.: Atmospheres*, 113(D13), 2008. doi:10.1029/2008JD009944.

[18] C. J. Kucharik and K. R. Brye. Integrated BIosphere Simulator (IBIS) Yield and Nitrate Loss Predictions for Wisconsin Maize Receiving Varied Amounts of Nitrogen Fertilizer. *J. Environ. Qual.*, 32:247—268, 2003. doi:10.2134/jeq2003.2470.

[19] W. Large and S. Yeager. The global climatology of an interannually varying air–sea flux data set. *Climate Dyn.*, 33(2–3):341–364, 2009. doi:10.1007/s00382-008-0441-3.

[20] D. M. Lawrence, K. W. Oleson, M. G. Flanner, C. G. Fletcher, P. J. Lawrence, S. Levis, S. C. Swenson, and G. B. Bonan. The CCSM4 land simulation, 1850-2005: Assessment of surface climate and new capabilities. *J. Climate*, 25(7):2240–2260, 2012. doi:10.1175/JCLI-D-11-00103.1.

[21] D. M. Lawrence, K. W. Oleson, M. G. Flanner, P. E. Thornton, S. C. Swenson, P. J. Lawrence, X. Zeng, Z.-L. Yang, S. Levis,

K. Sakaguchi, G. B. Bonan, and A. G. Slater. Parameterization improvements and functional and structural advances in Version 4 of the Community Land Model. *J. Adv. Model. Earth Syst.*, 3(3), 2011. doi:10.1029/2011MS000045.

[22] D. M. Lawrence, A. G. Slater, and S. C. Swenson. Simulation of Present-Day and Future Permafrost and Seasonally Frozen Ground Conditions in CCSM4. *J. Climate*, 25(7):2207–2225, 2011. doi:10.1175/JCLI-D-11-00334.1.

[23] S. Levis, G. B. Bonan, E. Kluzek, P. E. Thornton, A. Jones, W. J. Sacks, and C. J. Kucharik. Interactive crop management in the Community Earth System Model (CESM1): Seasonal influences on land-atmosphere fluxes. *J. Climate*, 25(14):4839–4859, 2012. doi:10.1175/JCLI-D-11-00446.1.

[24] X. Liu, R. C. Easter, S. J. Ghan, R. Zaveri, P. Rasch, X. Shi, J.-F. Lamarque, A. Gettelman, H. Morrison, F. Vitt, A. Conley, S. Park, R. Neale, C. Hannay, A. M. L. Ekman, P. Hess, N. Mahowald, W. Collins, M. J. Iacono, C. S. Bretherton, M. G. Flanner, and D. Mitchell. Toward a minimal representation of aerosols in climate models: description and evaluation in the Community Atmosphere Model CAM5. *Geosci. Model Dev.*, 5(3):709–739, 2012. doi:10.5194/gmd-5-709-2012.

[25] G. Madec and the NEMO team. *NEMO ocean engine*. Institut Pierre Simon Laplace, Nôte du Pole de Modèlisation 27, 2008. URL: http://www.nemo-ocean.eu/content/download/21612/97924/file/NEMO_book_3_4.pdf.

[26] H. Morrison and A. Gettelman. A new two-moment bulk stratiform cloud microphysics scheme in the Community Atmosphere Model, version 3 (CAM3). Part I: Description and numerical tests. *J. Climate*, 21(15):3642–3659, 2008. doi:10.1175/2008JCLI2105.1.

[27] R. B. Neale and Coauthors. Description of the NCAR Community Atmosphere Model (CAM 5.0). NCAR Technical Note NCAR/TN-486, National Center for Atmospheric Research, 2010. URL: http://www.cesm.ucar.edu/models/cesm1.1/cam/docs/description/cam5_desc.pdf.

[28] K. W. Oleson, G. B. Bonan, J. Feddema, M. Vertenstein, and C. Grimmond. An urban parameterization for a global climate model. Part I: Formulation and evaluation for two cities. *J. of Appl. Meteor. and Climatol.*, 47(4):1038–1060, 2008. doi:10.1175/2007JAMC1597.1.

[29] K. W. Oleson and Coauthors. Technical Description of version 4.0 of the Community Land Model (CLM). NCAR Technical Note NCAR/TN-478, National enter for Atmospheric Research, 2010. doi:10.5065/D6FB50WZ.

[30] S. Park and C. S. Bretherton. The University of Washington shallow convection and moist turbulence schemes and their impact on climate simulations with the Community Atmosphere Model. *J. Climate*, 22(12):3449–3469, 2009. doi:10.1175/2008JCLI2557.1.

[31] R. Pincus, H. W. Barker, and J.-J. Morcrette. A fast, flexible, approximate technique for computing radiative transfer in inhomogeneous cloud fields. *J. Geophys. Res.: Atmospheres*, 108(D13), 2003. doi:10.1029/2002JD003322.

[32] D. Rothrock. The energetics of the plastic deformation of pack ice by ridging. *J. Geophys. Res.*, 80(33):4514–4519, 1975. doi:10.1029/JC080i033p04514.

[33] G. Roullet and G. Madec. Salt conservation, free surface, and varying levels: A new formulation for ocean general circulation models. *J. Geophys. Res.: Oceans*, 105(C10):23927–23942, 2000. doi:10.1029/2000JC900089.

[34] W. Sacks, B. Cook, N. Buenning, S. Levis, and J. Helkowski. Effects of global irrigation on the near-surface climate. *Climate Dyn.*, 33(2-3):159–175, 2009. doi:10.1007/s00382-008-0445-z.

[35] R. Smith, P. Jones, B. Briegleb, F. Bryan, G. Danabasoglu, J. Dennis, J. Dukowicz, C. Eden, B. Fox-Kemper, P. Gent, et al. The parallel ocean program (POP) reference manual. Technical Report LAUR-10-01853, Los Alamos National Lab, 2010. URL: http://nldr.library.ucar.edu/repository/collections/OSGC-000-000-000-954.

[36] B. Tartinville, J.-M. Campin, T. Fichefet, and H. Goosse. Realistic representation of the surface freshwater flux in an ice–ocean general circulation model. *Ocean Modell.*, 3(1):95–108, 2001. doi:10.1016/S1463-5003(00)00017-2.

[37] A. S. Thorndike, D. A. Rothrock, G. A. Maykut, and R. Colony. The thickness distribution of sea ice. *J. Geophys. Res.*, 80(33):4501–4513, 1975. doi:10.1029/JC080i033p04501.

[38] P. E. Thornton, J.-F. Lamarque, N. A. Rosenbloom, and N. M. Mahowald. Influence of carbon-nitrogen cycle coupling on land model response to CO_2 fertilization and climate variability. *Global Biogeochem. Cycles*, 21(4), 2007. doi:10.1029/2006GB002868.

[39] M. Vancoppenolle, S. Bouillon, T. Fichefet, H. Goosse, O. Lecomte, M. A. Morales Maqueda, and G. Madec. *LIM The Louvain-la-Neuve sea ice model*. Institut Pierre Simon Laplace, Nôte du Pole de Modèlisation 31, 2012. URL: http://www.nemo-ocean.eu/content/download/21473/97362/file/Vancoppenolle_LIM3_book_NPM31_2012.pdf.

[40] C. S. Zender, H. Bian, and D. Newman. Mineral Dust Entrainment and Deposition (DEAD) model: Description and 1990s dust climatology. *J. Geophys. Res.: Atmospheres*, 108(D14), 2003. doi:10.1029/2002JD002775.